

Islanding of Methyl Radicals: A Key Factor in Hydrocarbon Chain Propagation Reactions

Ping Chuang,[†] Y. L. Chan,[‡] Shu-Hua Chien,[†] K.-J. Song,[§] Ruth Klauser,^{||} and T. J. Chuang^{*,†,§}

Center for Condensed Matter Sciences and Department of Physics, National Taiwan University, Taipei 106, Taiwan, Institute of Atomic and Molecular Sciences, Academia Sinica, Taipei, Taiwan, and Synchrotron Radiation Research Center, Hsinchu, Taiwan

Received January 3, 2002. In Final Form: March 25, 2002

A sequence of long-chain alkene products is found to evolve from chemisorbed methyl groups on Cu(111) in temperature-programmed reaction. The results of low-energy electron diffraction measurements suggest the formation of 2D islands for the chemisorbed radicals. The close-packed adsorption geometry and the reaction kinetics to generate high mass species are closely correlated. From this and other studies, we infer that the tendency of the methyl radicals to aggregate even at submonolayer coverages is crucial in promoting the chain growth, and the observed islanding effect may be significant in other hydrocarbon catalytical systems.

Introduction

There exist numerous attempts to mimic heterogeneous catalysis under well-controlled ultrahigh vacuum conditions, in order to understand the basic reaction steps and mechanisms.^{1–3} A number of recent studies^{3–9} have shown remarkably that long-chain hydrocarbons can be produced from single carbon radical species adsorbed on single-crystal metal surfaces, resembling important aspects of the well-known Fischer–Tropsch reactions. The investigations have yielded certain insight into the general reaction schemes, but a full account of the crucial factors controlling the reaction rates and product branching ratios is still lacking. In particular, the adsorbate structures and lateral effects have rarely been considered in prior works. Recently, there has been growing interest in understanding the influence of adsorbate–adsorbate interaction and island formation on surface reaction kinetics. A well-known system exhibiting the islanding behavior is the CO oxidation reaction which has been studied both theoretically and experimentally.^{10–12} Likewise, the oxidation of methyl formate was demonstrated to occur quite localized at the end of (2 × 1)O rows on Cu(110).¹³ The effects of adsorbate aggregation on thermal desorption spectra of nitrogen were also examined.¹⁴ It

appears, however, that in the hydrocarbon surface chemistry, the islanding phenomenon of CH_x radicals and its effect on the chain propagation reactions have never been reported. We present here some striking observations on Cu(111) surface exposed to methyl (CH₃) radicals to shed some light into the problem. It was found not only that a series of high mass alkyl products can be generated in a relatively mild thermal process but also that they can evolve from the metal surface all at the same temperature. Furthermore, such reactions can take place even at a very small surface coverage. By examining the adsorbate–surface topographic structure as a function of surface coverage and temperature, and correlating the structure with the thermal chemistry, we conclude that islanding of the chemisorbed methyl radicals must play a key role in facilitating the chain propagation process. To our knowledge, it is the first observation of two-dimensional island formation on a metal surface exposed to such radicals.

Experimental Section

The experiments were carried out in an ultrahigh vacuum system equipped with a high-resolution electron energy loss spectrometer (HREELS), X-ray photoemission (XPS), temperature-programmed desorption (TPD) with a quadrupole mass spectrometer (QMS), and low-energy electron diffraction (LEED) as described previously.^{15,16} Methyl radicals were generated from azomethane gas passed through a hot quartz nozzle source^{8,9,15–18} and dosed directly onto the Cu(111) surface. The adsorbed hydrocarbons were analyzed by XPS and HREELS, the surface structure by LEED, and the gaseous products by TPD. The total adsorbate coverage (θ) averaged over the sample surface was determined quantitatively by the attenuation of Cu 2p XPS signal¹⁶ and from TPD spectra. For LEED measurements, the charge deposition on the sample was carefully controlled to minimize the electron irradiation effect, and the patterns were recorded by a CCD camera.

* Corresponding author. Fax: +886-2-2365-5404. E-mail: chuangtj@ccms.ntu.edu.tw.

[†] Department of Chemistry.

[‡] Center for Condensed Matter Sciences.

[§] Institute of Atomic and Molecular Sciences.

^{||} Synchrotron Radiation Research Center.

(1) Zaera, F. *Chem. Rev.* **1995**, *95*, 2651.

(2) Somorjai, G. A. *Chem. Rev.* **1996**, *96*, 1223.

(3) Bent, B. E. *Chem. Rev.* **1996**, *96*, 1361.

(4) Chiang, C. M.; Bent, B. E. *Surf. Sci.* **1992**, *279*, 79.

(5) Lin, J. L.; Bent, B. E. *J. Vac. Sci. Technol., A* **1992**, *10*, 2202.

(6) Chiang, C. M.; Wentzclaff, T. H.; Bent, B. E. *J. Phys. Chem.* **1992**, *96*, 1836.

(7) Lin, J. L.; Chiang, C. M.; Jenks, C. J.; Yang, M. X.; Wentzclaff, T. H.; Bent, B. E. *J. Catal.* **1994**, *147*, 250.

(8) Kim, S. H.; Stair, P. C. *J. Am. Chem. Soc.* **1998**, *120*, 8535.

(9) Kim, S. H.; Stair, P. C. *J. Phys. Chem. B* **2000**, *104*, 3035.

(10) Hellsing, B.; Zhdanov, V. P. *Chem. Phys. Lett.* **1988**, *147*, 613.

(11) Silverberg, M.; Ben-Shaul, A. *Chem. Phys. Lett.* **1987**, *134*, 491.

(12) Winterlin, J.; Volkening, S.; Janssens, T. V. W.; Zambelli, T.; Ertl, G. *Science* **1997**, *278*, 1931.

(13) Silva, S. L.; Patel, A. A.; Pham, T. M.; Leibsle, F. M. *Surf. Sci.* **1999**, *441*, 351.

(14) Hood, E. S.; Toby, B. H.; Weinberg, W. H. *Phys. Rev. Lett.* **1985**, *55*, 2437.

(15) Chan, Y. L.; Chuang, P.; Chuang, T. J. *J. Vac. Sci. Technol., A* **1998**, *16*, 1023.

(16) Chuang, T. J.; Chan, Y. L.; Chuang, P.; Klauser, R. *J. Electron Spectrosc. Relat. Phenom.* **1999**, *98/99*, 149.

(17) Peng, X. D.; Viswanathan, R.; Smudde, G. H. J.; Stair, P. C. *Rev. Sci. Instrum.* **1992**, *63*, 3930.

(18) Dickens, K. A.; Stair, P. C. *Langmuir* **1998**, *14*, 1444.

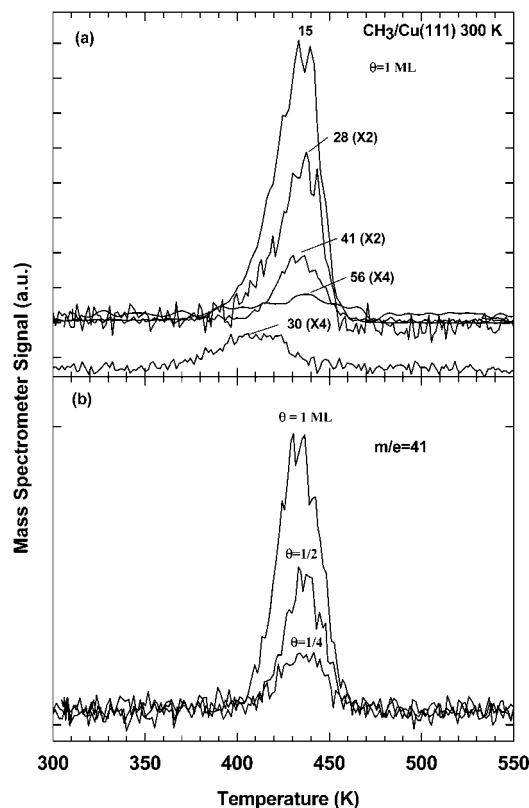


Figure 1. TPD spectra: (a) monitoring $m/e = 15$ (CH_4), 28 (C_2H_4), 30 (C_2H_6), 41 (C_3H_6), and 56 (C_4H_8) signals for adsorbed CH_3 with 1 monolayer coverage on Cu(111) at 300 K; (b) monitoring $m/e = 41$ (C_3H_6) signals at 0.25, 0.5, and 1.0 monolayer CH_3 surface coverages.

Results and Discussion

As shown in our prior work,^{15,16} $\text{CH}_3(\text{ads})$ chemisorption is readily detected by XPS and HREELS when the clean Cu(111) surface at 300 K is exposed to the radical source. There is no N-containing species or any other contaminant. The chemisorption of the radicals, however, is accompanied by some dissociation into $\text{CH}_2(\text{ads})$ and $\text{H}(\text{ads})$, possibly around the surface defect sites. Figure 1a depicts the TPD spectra for various masses when a monolayer ($\theta = 1$ monolayer, saturation coverage at 300 K, invariable with the amount of CH_3 exposure) of adsorbates is heated at 3 K/s from 300 to 600 K. The primary gaseous products are CH_4 , C_2H_4 , C_2H_6 , C_3H_6 , and C_4H_8 molecules. The molecular entities of these species are determined by measuring the relative signal intensities at various masses and comparing those with the cracking patterns of known molecules by our quadrupole mass spectrometer. For instance, mass signals at 26, 27, and 28 amu are used to identify C_2H_4 , 39, 41, and 42 amu for C_3H_6 (propylene), and 41 and 56 amu for C_4H_8 (1-butene). At a submonolayer coverage, the high mass species (C_3H_6 and C_4H_8) are still detectable, although the signal strengths are substantially weaker. Figure 1b exhibits the TPD signals for C_3H_6 as a function of surface coverage (θ in monolayers). Clearly C_3H_6 can be produced even at $\theta \leq 0.2$ monolayers. It is worth noting that butene or a higher mass product has never been observed in prior works for CH_3/Cu systems with CH_3I as the reagent.³⁻⁷ Furthermore, our TPD spectra always exhibit a single desorption peak for all hydrocarbon species at all gaseous exposures. This fact shows that at saturation coverage, θ is indeed 1 monolayer and there is no multilayer adsorption.

The results show remarkably that long-chain alkenes can be readily produced from chemisorbed CH_3 radicals all at the same time in a temperature ramp. In the present system, we find that CH_4 , C_2H_4 , C_3H_6 , and C_4H_8 products are generated at the same temperature of 437 K (± 3 K) under the given condition. Moreover, the peak desorption temperature is independent of initial CH_3 surface coverage. This implies the first-order reaction kinetics for those products. In contrast, the TPD peak for C_2H_6 is around 410 K (also displayed in Figure 1a), and this value shifts from 420 K at $\theta = 0.3$ monolayer to 408 K at $\theta = 1$ monolayer. The reaction and desorption exhibit the characteristics of second-order kinetics, and the product is apparently due to the direct coupling of two $\text{CH}_3(\text{ads})$ radicals. In prior studies on Cu surfaces by Bent et al.³⁻⁷ with CH_3I as the source for CH_3 radicals, CH_4 , C_2H_4 , and C_3H_6 production and desorption were detected at 450 K on Cu(111)⁵ and at 470 K on Cu(100)⁷ independent of surface coverage. For CH_3 generated the same way as the present study but adsorbed on oxygen-modified Mo(100), Kim and Stair^{8,9} reported the formation of CH_4 , C_2H_4 , C_3H_6 , C_4H_8 , and C_5H_{10} at nearly the same temperature of 440 K. Apparently, in all these $\text{CH}_3/\text{surface}$ systems, there are common molecular production, desorption characteristics, and reaction kinetics. In the previous investigations, it was proposed that some $\text{CH}_3(\text{ads})$ radicals were decomposed to form $\text{CH}_2(\text{ads})$ groups which subsequently reacted with intact CH_3 to generate C_{2+} alkyl products. Specifically, Bent's research group has suggested CH_3 dissociation by α -elimination of a hydrogen atom to be the rate-limiting step for the chain reactions. Namely, the reaction scheme can be represented by $\text{CH}_3(\text{ads}) \rightarrow \text{CH}_2(\text{ads}) + \text{H}(\text{ads})$, followed by $\text{CH}_3(\text{ads}) + \text{H}(\text{ads}) \rightarrow \text{CH}_4(\text{g})\uparrow$ and $\text{CH}_3(\text{ads}) + \text{CH}_2(\text{ads}) \rightarrow \text{C}_2\text{H}_5(\text{ads}) \rightarrow \text{C}_2\text{H}_4(\text{g})\uparrow + \text{H}(\text{ads})$. Subsequently, the C_3 product can be generated by $\text{C}_2\text{H}_5 + \text{CH}_2 \rightarrow \text{C}_3\text{H}_7 \rightarrow \text{C}_3\text{H}_6(\text{g})\uparrow + \text{H}$, and by extension higher mass species can be formed by $\text{C}_3\text{H}_7 + \text{CH}_2 \rightarrow \text{C}_4\text{H}_9 \rightarrow \text{C}_4\text{H}_8(\text{g})\uparrow + \text{H}$, ..., etc. In other words, there is a sequential methylene insertion at the α -carbon position into the transient alkyl species to produce longer carbon chains. There is experimental evidence to support such a reaction scheme.³⁻⁹ It should be noted that according to the scheme, the fate of the transient species such as C_2H_5 and C_3H_7 is either desorption by dehydrogenation or reaction with another CH_2 for the chain growth. The critical question to ask in the present as well as previous systems is why the reactions leading to the C_{3+} alkyl products can occur all at nearly the same temperature and independent of surface coverage. We have detected C_3H_6 formation even at θ less than 0.2 monolayer. How can this take place via the sequential reaction process when the surface is, on the average, so sparsely occupied by the radicals?

To resolve this puzzle, we decided to look further into the adsorption geometry and dynamic behavior of CH_3 radicals on Cu(111) by use of the LEED technique. Panels a and b of Figure 2 depict the LEED patterns at $\theta = 0.25$ and 1.0 monolayers with Cu(111) at 300 K. At saturation coverage, the LEED pattern exhibits six bright spots indicative of $(\sqrt{3} \times \sqrt{3})\text{R}30^\circ$ superstructure. In addition, there is a dim hexagon-like structure connecting the $(\sqrt{3} \times \sqrt{3})\text{R}30^\circ$ spots. This pattern of discrete spots with the diffuse hexagon structure is still clearly visible at 380 K (Figure 2c) and even momentarily at 420 K (Figure 2d). At 450 K or higher, the LEED intensity due to the adsorbate disappears when the reaction is completed. As the initial θ decreases, the spots due to $(\sqrt{3} \times \sqrt{3})\text{R}30^\circ$ superstructure fade away while the diffuse hexagon pattern gains intensity. For low coverage samples with only a diffuse hexagon pattern at 300 K, cooling to 120 K

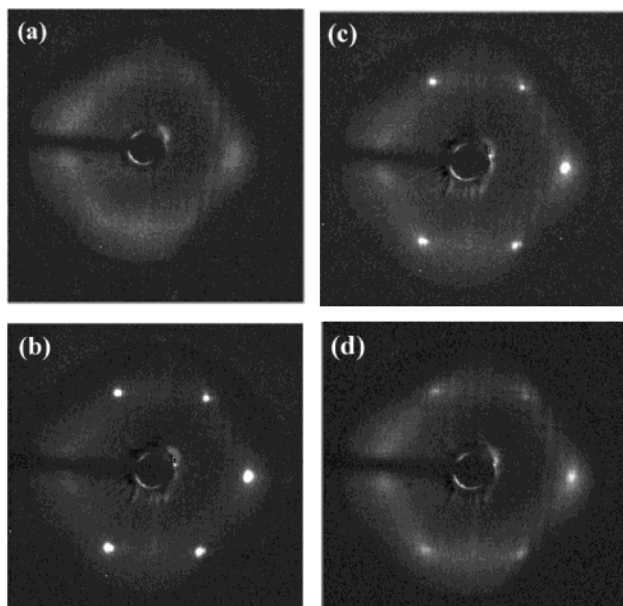


Figure 2. LEED (e-beam energy $E = 30$ eV) patterns of CH_3 on Cu(111) at 300 K with CH_3 coverages of (a) $\theta = 0.25$ monolayer and (b) $\theta = 1.0$ monolayer. The temperature of sample (b) is then raised to 380 K (c) and 420 K (d).

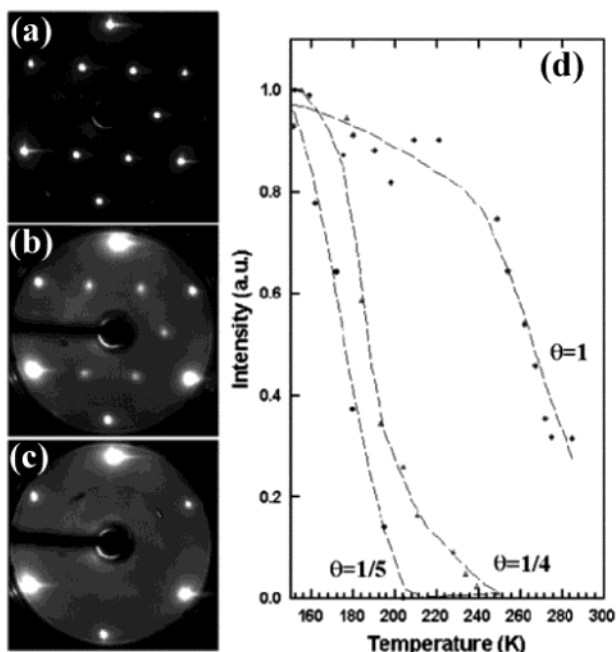


Figure 3. LEED ($E = 67$ eV) patterns of $\theta = 0.3$ monolayer of CH_3 on Cu(111) at 120 K (a) and raised to 210 K (b) and 300 K (c). The intensities of (a) and (c) are amplified by a factor of 2 to show the details. The bright spots at outermost positions (six spots) are from Cu(111) substrate. These substrate diffraction spots are visible on a LEED screen with $E = 67$ eV (but invisible with $E = 30$ eV as in Figure 2). (d) Sum of the spots intensities of $(\sqrt{3} \times \sqrt{3})R30^\circ$ structure as a function of temperature at various CH_3 coverages as indicated.

causes the $(\sqrt{3} \times \sqrt{3})R30^\circ$ spots to show up. The LEED patterns with $\theta = 0.3$ monolayer at various temperatures are displayed in panels a–c of Figure 3. Such a transition is reversible. If the sample temperature is raised again, the discrete spots fade away while the hexagon pattern becomes more pronounced. As shown in Figure 3d, the temperature range where the discrete spots disappear depends strongly on coverage. The higher the coverage,

the higher the temperature the discrete spots can survive. The transition temperature (i.e., at the point that the intensity of a discrete spot decreases to one-half of its low T value) also depends on the annealing history of the sample, being higher if the sample has been annealed at a higher temperature. It should be mentioned clearly that θ remains constant when the substrate T is varied between 120 and 350 K.

To interpret the LEED data, we have to consider the size of a methyl group and its possible adsorption geometry. Note that the van der Waals diameter of 4 Å for a methyl group is much larger than the nearest neighbor Cu–Cu distance of 2.55 Å. It is thus inevitable to cause space hindrance if one tries to put more than one methyl radical into one $(\sqrt{3} \times \sqrt{3})R30^\circ$ unit cell. Our ab initio calculations indicate that adsorption of two methyl radicals per $(\sqrt{3} \times \sqrt{3})R30^\circ$ unit cell is possible, but the adsorption energy per methyl is reduced by a large amount of 0.6 eV (compared with one methyl per unit cell case). In such “doubly packed” geometry, the CH_3 groups cannot freely rotate. Thus, a less densely packed structure is clearly favored. Since cooling a low-coverage sample can cause spontaneous conversion to the $(\sqrt{3} \times \sqrt{3})R30^\circ$ structure, this strongly suggests that the $(\sqrt{3} \times \sqrt{3})R30^\circ$ structure formed by cooling has only one methyl per unit cell.

At θ below 0.5 monolayer, we always obtain LEED patterns with a diffuse hexagon at 300 K. Close inspection of the hexagons reveals that they only have 3-fold rotational symmetry. The diffuse nature of the pattern suggests the real space structure to be highly disordered. At this stage, few specifics of this structure are known. We postulate that the structure consists of two-dimensional (2D) islands of “liquidlike” (i.e., highly disordered but condensed) methyl radicals. It is well-known that the melting temperature of 3D clusters reduces significantly as their sizes become smaller.¹⁹ It is thus plausible to postulate the transition temperature between the 2D liquidlike phase, and the ordered $(\sqrt{3} \times \sqrt{3})R30^\circ$ phase also reduces significantly as the size of the 2D islands shrinks. It is well established that the growth of an epitaxial film proceeds first through a nucleation stage and then through a growth stage.²⁰ In the growth stage, the number of islands quite often stays fixed while each island grows in size as deposition proceeds. The average size of the 2D islands is determined by the average coverage divided by the fixed number density of islands, and therefore it is proportional to the coverage. From this consideration, the observed higher transition temperature for higher coverage can be easily understood as due to the larger island size.

Even after deposition, if surface diffusion is effective at the given temperature, the islands can undergo coarsening²¹ in which the average size of the 2D islands gradually increases. Such increase is especially prominent when the sample temperature is raised to a high level below the onset of thermal desorption. Thus one would predict that the order–disorder transition temperature of the methyl-covered surface to be an increasing function of the maximum temperature the sample has ever been annealed at. This prediction turns out to be true. For instance, we have prepared a sample by dosing at 265 K until $\theta = 0.3$ monolayer and then cooled to 120 K. With the sample heated slowly, the transition temperature is found to be 207 K. The same sample is then annealed at 320 K and

(19) Lai, S. L.; Guo, J. Y.; Petrova, V.; Ramanath, G.; Allen, L. H. *Phys. Rev. Lett.* **1996**, *77*, 99.

(20) Thiel, P. A.; Evans, J. W. *J. Phys. Chem.* **2000**, *104*, 1663.

(21) Pai, W. W.; Swan, A. K.; Zhang, Z.; Wendelken, J. F. *Phys. Rev. Lett.* **1997**, *79*, 3210.

cooled to 120 K. By heating at the same rate again, the transition temperature is now found to be 217 K. This increase supports the idea that the methyl radicals have a natural tendency to aggregate into ever larger 2D islands at higher temperatures. Furthermore, we have investigated the tendency of islanding even when the methyl radicals have enough energy to react. For a sample with near saturation coverage, we find the integrated intensity of the hexagon increases with T , reaches the maximum around 400–440 K, and then finally disappears completely when all the hydrocarbon radicals are depleted by the thermal reactions and desorption. This temperature range of 400–440 K is exactly the same as that of long-chain alkyl production detected by TPD (Figure 1). Thus, the disordered phase indeed can survive at the reaction temperature.

The ability to form 2D islands for the radical adsorbates regardless of the total surface coverage seems to be crucial for the alkyl chain propagation reactions. In the proposed scheme for C_3H_6 and C_4H_8 production via CH_2 insertion mechanism, the transient $C_2H_5(ads)$ and $C_3H_7(ads)$ species have to react effectively with $CH_2(ads)$ within their relatively short lifetimes, in competition with the desorption channel. If the chemisorbed $CH_3(ads)$ and $CH_2(ads)$ radicals were to reside sparsely and far away from the transient species, there would be little chance for the formation of C_{3+} species. Surface diffusion could be too slow for the reaction process. In the 2D island structure, the radicals are close neighbors even at a very small

(average) surface coverage. Such adsorption geometry can greatly enhance the chemical reactivity.

Conclusion

In the temperature-programmed reaction and desorption measurements, a series of high mass hydrocarbon products, up to C_4H_8 , are observed from the chemisorbed $CH_3(ads)$ groups on Cu(111). The long-chain alkyl species evolve from the surface all at the same temperature and independent of the initial surface coverage (≤ 1 monolayer). Such reaction behavior and kinetics can be understood based on a close-packed adsorption geometry which is verified by LEED measurements. The study shows that $CH_3(ads)$ groups tend to aggregate in forming 2D islands with $(\sqrt{3} \times \sqrt{3})R30^\circ$ structure even at submonolayer coverages. The close proximity of the reactants is apparently essential in facilitating the chain propagation reactions initiated by $CH_2(ads)$ formation followed by the methylene insertion process. We therefore conclude that the islanding behavior is a key factor in promoting chain reactions to generate high mass alkyl products. The observed effect may have a wide implication in heterogeneous catalysis.

Acknowledgment. The authors wish to thank the National Science Council and the Ministry of Education of R.O.C. for support of this work.

LA020016Y